



## Original article

## Three-dimensional quantitative structure–selectivity relationships analysis guided rational design of a highly selective ligand for the cannabinoid receptor 2

Simone Brogi<sup>a</sup>, Federico Corelli<sup>a</sup>, Vincenzo Di Marzo<sup>b</sup>, Alessia Ligresti<sup>b</sup>, Claudia Mugnaini<sup>a</sup>, Serena Pasquini<sup>a</sup>, Andrea Tafi<sup>a,\*</sup>

<sup>a</sup> Dipartimento Farmaco Chimico Tecnologico, Università degli Studi di Siena, Via Alcide de Gasperi 2, 53100 Siena, Italy

<sup>b</sup> Endocannabinoid Research Group, Institute of Biomolecular Chemistry, Consiglio Nazionale delle Ricerche, Via dei Campi Flegrei 34, 80078 Pozzuoli (Napoli), Italy

## ARTICLE INFO

## Article history:

Received 6 August 2010

Received in revised form

22 October 2010

Accepted 19 November 2010

Available online 27 November 2010

## Keywords:

3D-QSSR

Cannabinoid receptor 2

Selective ligands

Computer-aided drug design

Quinolones

## ABSTRACT

This paper describes a three-dimensional quantitative structure–selectivity relationships (3D-QSSR) study for selectivity of a series of ligands for cannabinoid CB1 and CB2 receptors. 3D-QSSR exploration was expected to provide design information for drugs with high selectivity toward the CB2 receptor. The proposed 3D computational model was performed by Phase and generated taking into account a number of structurally diverse compounds characterized by a wide range of selectivity index values. The model proved to be predictive, with  $r^2$  of 0.95 and  $Q^2$  of 0.63. In order to get prospective experimental validation, the selectivity of an external data set of 39 compounds reported in the literature was predicted. The correlation coefficient ( $r^2 = 0.56$ ) obtained on this unrelated test set provided evidence that the correlation shown by the model was not a chance result. Subsequently, we essayed the ability of our approach to help the design of new CB2-selective ligands. Accordingly, based on our interest in studying the cannabinergic properties of quinolones, the *N*-(adamantan-1-yl)-4-oxo-8-methyl-1-pentyl-1,4-dihydroquinoline-3-carboxamide (**65**) was considered as a potential synthetic target. The log(SI) value predicted by using our model was indicative of high CB2 selectivity for such a compound, thus spurring us to synthesize it and to evaluate its CB1 and CB2 receptor affinity. Compound **65** was found to be an extremely selective CB2 ligand as it displayed high CB2 affinity ( $K_i = 4.9$  nM), while being devoid of CB1 affinity ( $K_i > 10,000$  nM). The identification of a new selective CB2 receptor ligand lends support for the practicability of quantitative ligand-based selectivity models for cannabinoid receptors. These drug discovery tools might represent a valuable complementary approach to docking studies performed on homology models of the receptors.

© 2010 Elsevier Masson SAS. All rights reserved.

### 1. Introduction

The cannabinoid 1 receptor (CB1 receptor) and the cannabinoid 2 receptor (CB2 receptor) are members of the G-protein-coupled receptor family [1]. While CB1 receptor is abundantly expressed in the central nervous system (CNS), CB2 receptor is mainly localized in peripheral nerve terminals and in the tissues of the immune system [2]. Recent studies have suggested that CB2 receptor is also expressed in certain subpopulations of the CNS and evidence is growing that CB1 receptor is also expressed in peripheral tissues [3].

Agonists of both cannabinoid receptor subtypes produce strong antinociceptive effects in animal models of chronic, neuropathic,

and inflammatory pain and are intensively investigated as potential new analgesic and antiinflammatory agents [4]. Unfortunately, CB1/CB2 agonists are not devoid of unwanted side effects, many of which are thought to be due to activation of central CB1 receptor rather than peripheral CB1 or CB2 receptors [5].

In principle, separating the therapeutic effects of cannabinoid agonists from their undesired effects could be accomplished by either preventing the ligands from crossing the blood–brain barrier or by increasing the selectivity of the ligands for the CB2 receptor [6]. Several classes of selective CB2 ligands have demonstrated efficacy in pre-clinical models of inflammatory pain [7] and have shown a therapeutic window with regard to CNS side effects [8]. However, none of the CB2-selective agonists that have been developed to date are completely CB2-specific. Thus, they are all expected to display CB2 selectivity only within a finite dose range and to target CB1 receptor as well when administered at a dose that lies above this range [9]. On the basis of these considerations,

\* Corresponding author. Tel.: +39 0577 234 313; fax: +39 0577 234 333.

E-mail address: [tafi@unisi.it](mailto:tafi@unisi.it) (A. Tafi).

interest is growing in developing new structural classes of CNS penetrant CB2 agonists with high receptor subtype selectivity suitable for *in vivo* studies [6,10–12].

Even though many efforts have been directed in recent years to the modeling of CB2 receptor binding, the rational design of novel CB2-selective ligands by computational methodologies is still a challenging task [10]. The vast majority of computational studies on CB receptors consist either of retrospective rationalizations focused on protein–ligand docking simulations using homology models of both receptors and 3D-QSAR models [13], or in pharmacophore-based virtual screening protocols [14]. Hence, a lack is perceived of predictive models for CB2 selectivity, effective to assist the drug design process. On the other hand, the knowledge of several CB2-selective classes of compounds might allow pharmacophore modeling (PM) to help fill this gap. This technique, in fact, not only enables fast design of novel structural scaffolds, but also provides sound alignment rules whereon one could ground predictive three-dimensional structure–selectivity relationships (3D-QSSR) approaches.

The difficulties inherent in the rational discovery of selective ligands of CB2 receptor with a clear-cut functional activity profile (agonist/antagonist/inverse agonist) have been recently faced in the case of pharmacophore modeling [14]. Markt and coworkers demonstrated that CB2 receptor-selective agonists and antagonists/inverse agonists can be “structurally closely related” so that “the differences in terms of chemical features are subtle”. Consequently, these authors have abandoned the idea of generating selective models for agonists, antagonists and inverse agonists as “discrimination between agonists and antagonists would only be possible with very restrictive pharmacophore models which would not be suitable for a virtual screening workflow focused on the discovery of structurally novel scaffolds” [14]. Actually, the pharmacophore model developed by these authors, though based on CB2 receptor-selective agonists only, screened some ligands with moderate selectivity, different binding behavior and functional activity.

Up to date, only a CoMFA/CoMSIA model of selectivity for indole ligands of CB1 and CB2 receptor subtypes has been published, in which the functional activities of the studied set of compounds (generally proposed as agonists) have not been analyzed in detail [15]. A general strategy for the development of selectivity models, however, has been recently suggested by Weber and coworkers through CoMFA/CoMSIA analyses of inhibitors of carbonic anhydrase isoforms. These scientists have derived the molecular alignment of isozyme selective inhibitors from one enzyme isoform only, by molecular docking studies of compounds into its binding site [16]. An analogous approach can be applied in the case of CB1 and CB2 receptors, as the high degree of homology (68%) exhibited by the transmembrane domains of these targets causes binding affinities of their respective ligands to be generally correlated. Such an outcome, in fact, has been even evaluated to be consistent with the hypothesis that non selective compounds can keep the same conformation when bound to both subtypes [17]. Moreover, Wiley and coworkers have accounted for structure–activity relationships results suggesting the overlap, albeit incomplete, of the pharmacophores for CB1 and CB2 receptors [18].

Based on all the above considerations, we have developed an inclusive 3D-QSSR model, founded on a CB2 common feature pharmacophore and able to predict in a semi quantitative manner the selectivity index (see below) of novel CB2 receptor ligands belonging to several structural classes. According to the difficulties discussed above in the prediction of functional activity at CB2 receptor [14], in this study no analysis of ligands functional activities was performed. On the other hand the functional activity of several CB2 ligands reported so far in the literature and used in this study has been not explicitly determined [7c,19–27] so that they

might show a functional profile [28] different from that assigned by structural similarity [13c]. Phase [29], a software package designed for pharmacophore modeling, structure alignment and activity prediction has been used for this purpose. Notably, this package provides the means to align sets of ligands onto a pharmacophore and to develop 3D-QSAR models able to identify further structural features that govern molecule activity. In this study, Phase was firstly applied to develop a common feature CB2 pharmacophore model to be used as an alignment rule and, then, to carry out a 3D-QSSR investigation [30].

## 2. Results and discussion

A representative set of 64 CB2 ligands was selected (see Fig. 1 and Table S1), taking in no account their functional activity, among a number of 4-quinolone-3-carboxamides recently synthesized in our laboratory (**23–39** and **64**) [31] and derivatives belonging to different structural classes already reported in the literature (**1–13**, **17** and WIN55212-2 (**58**) [28], JWH-015 (**14**) and CP-55,940 (**55**) [32], JWH-181 (**15**) and JWH-007 (**16**) [19], AM1241 (**18**) [33], AM630 (**19**) [34], **20–22** and **40–42** [7c], **43–45** [20], L759633 (**46**) and L759656 (**47**) [35], **48–51** [21], O-1057 (**52**) [36], AMG41 (**53**) [22], JWH-133 (**54**) [23], AM855 (**56**) [24], BAY593074 (**57**) [37], gp1a (**59**) [38], **60** [39], SR144528 (**61**) [40], HU-308 (**62**) [41], and GW405833 (**63**) [42]). The binding affinities of all these compounds for human recombinant CB1 and CB2 receptors ( $K_i$  values) have been measured according to the same protocol, by displacement of the radioligand [ $^3$ H]-CP-55,940 [7c,19–24,28,31–42] and are shown in Table 1 (second and third columns).

Our selection was restrained to compounds showing high CB2 affinity ( $K_i$  values  $\leq 56.7$  nM) and CB1 affinity covering approximately four orders of magnitude ( $K_i$  values ranging from 0.5 to  $>10,000$  nM). As a consequence, the selectivity index of the compounds [SI, calculated as  $K_i(\text{CB1})/K_i(\text{CB2})$  ratio, fourth column of Table 1] essentially depends on their affinity at CB1 receptor. With the aim to develop a bare selectivity model, the  $\log(\text{SI})$  was used as the experimental activity variable in Phase. The selectivity index of some derivatives (“undetermined” compounds hereafter) was not computable precisely due to their low CB1 affinity [ $K_i(\text{CB1}) > 10,000$  nM]. However, because highly selective compounds were considered as a source of important structure–selectivity relationships, two “undetermined” compounds (**20** and **24**) were included in the training set, with a 10,000 nM  $K_i(\text{CB1})$  value arbitrarily assigned, in order to avoid the loss of positive information. The remainder of the undetermined compounds was included in the test set to stress the model predictivity. Therefore, the dependent QSSR variable spanned a four logarithmic units range starting from zero, ensuring statistical significance to the approach.

All the compounds were aligned onto a purpose-built CB2 common feature pharmacophore (details concerning the building of the pharmacophore and its performance as a retrospective 3D-QSAR modeling tool are provided in Supplementary material). Three quantitative selectivity models containing one to three PLS factors were then generated. Due to the peculiarity of our purpose and according to Phase manual suggestions, the atom-based version of the QSAR methodology was preferred to the pharmacophore-based one, in order to consider contributions to selectivity possibly deriving from features other than the pharmacophore [30]. The whole set of 64 molecules was divided into a training set and a test set represented by 29 and 35 compounds (Table 1), respectively, selected in an unbiased way in an effort to maximize structural diversity and coverage of experimental activities. Compounds **20**, **24** and **59** represented the high boundary of our training set selectivity range.

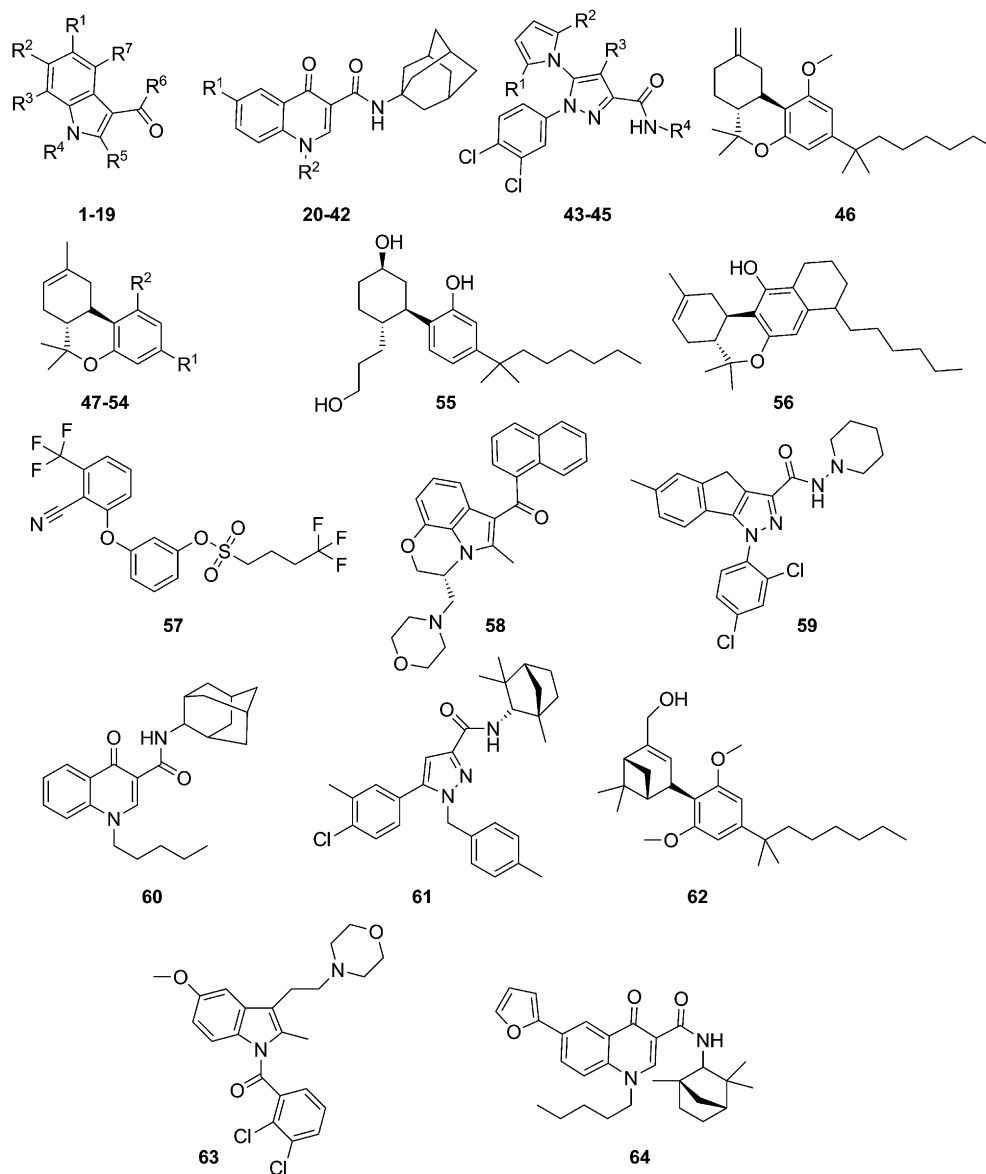


Fig. 1. Chemical scaffolds of the compounds used to generate the 3D-QSSR model (see Table S1 in the Supplementary material for further details).

Table 2 shows the statistical parameters derived using Phase methodology. The model with three PLS factors was preferred and chosen as the 3D-QSSR model, since it performed better on the whole than those with fewer factors. The correlation coefficients of the model ( $r^2 = 0.95$  and  $Q^2 = 0.63$ ) were statistically acceptable when considering both the ratio (0.8) between the number of compounds in the training and test sets, respectively, and the number of undetermined compounds included in the test set (11 compounds). Moreover, the high Pearson-R value (Pearson-R = 0.81) also indicated a close correlation between predicted and actual selectivity index values. These features, together with the small number of PLS factors, the large  $F$  value and the small variance ratio ( $P$ ) supported the robustness of the approach. The linear plot of calculated/predicted versus actual selectivity index values is displayed in Fig. 2 and reported in the fifth and fourth columns of Table 1. Notably, with the exception of **48**, the differences between experimental and calculated values were within one order of magnitude for all the compounds, demonstrating that the selectivity of compounds in both training and test sets was reasonably well estimated by the model.

The 3D-QSSR results were visualized using 3D plots of the crucial volume elements occupied by ligands. Figs. 3–5 show the 3D plot representation of the model as a whole superimposed to **24**, **61** (SR144528), and **55** (CP-55,940), respectively. In this representation blue and red cubes indicate positive and negative coefficients, respectively, that is volumes in which the occupying atoms of the ligands cause an increase or a decrease of selectivity. Cubes having small positive and negative coefficients, which therefore did not greatly affect selectivity, were filtered out by setting a  $\pm 2.0 \times 10^{-2}$  coefficient threshold. Notably, compound **24**, showing the greatest CB2 selectivity, mainly occupies blue regions, while the less CB2-selective derivative **61** occupies some of the red regions. Finally, derivative **55**, a compound showing no CB2 selectivity, mainly occupies red regions. In Fig. 6 only the cubes occupied by compound **24** are displayed, decomposed into the contributions to the model by different atom classes. The map corresponding to electron-withdrawing atoms (including hydrogen-bond acceptors) is displayed on the left of Fig. 6, while that corresponding to hydrophobic/non-polar atoms is shown on the right.

**Table 1**

CB1 and CB2 receptor affinity values [Ki(CB1) and Ki(CB2) columns, nM], experimental (Exp column) and estimated (Calc column) selectivity index values [log(SI)] for compounds used in the computational study. Estimated log(SI) values were calculated by application of 3D-QSSR model (see text).

Cmpd	Ki(CB1)	Ki(CB2)	Exp log(SI)	Calc log(SI)
1 <sup>a</sup>	45	0.1	2.57	2.49
2 <sup>a</sup>	845	4.4	2.30	2.30
3 <sup>a</sup>	228	0.4	2.27	2.18
4 <sup>b</sup>	33	0.9	1.58	1.80
5 <sup>b</sup>	28	0.2	2.30	2.02
6 <sup>b</sup>	3310	30.0	2.05	2.06
7 <sup>b</sup>	1700	25.0	1.85	1.86
8 <sup>a</sup>	1000	9.0	2.05	2.10
9 <sup>b</sup>	2951	8.3	2.55	1.59
10 <sup>b</sup>	280	4.6	2.00	1.97
11 <sup>b</sup>	234	1.3	2.30	1.84
12 <sup>b</sup>	780	0.7	3.05	2.46
13 <sup>a</sup>	28	3.0	0.98	0.93
14 (JWH-015) <sup>a</sup>	383	13.3	1.47	1.15
15 (JWH-181) <sup>a</sup>	1.3	0.6	0.32	0.08
16 (JWH-007) <sup>b</sup>	9.5	2.9	0.28	0.67
17 <sup>b</sup>	3500	32.0	2.05	1.94
18 (AM1241) <sup>a</sup>	5000	11.5	2.64	2.63
19 (AM630) <sup>b</sup>	5152	31.2	2.22	1.72
20 <sup>a</sup>	>10,000	3.8	3.42	3.2
21 <sup>a</sup>	42	4.7	0.95	1.20
22 <sup>a</sup>	2520	11.6	2.34	2.66
23 <sup>b</sup>	2080	20.6	2.01	2.06
24 <sup>a</sup>	>10,000	0.7	4.15	3.28
25 <sup>b</sup>	>10,000	2.3	3.68	2.88
26 <sup>b</sup>	>10,000	4.2	3.38	3.09
27 <sup>b</sup>	>10,000	8.3	3.08	2.20
28 <sup>b</sup>	>10,000	11.0	3.00	3.11
29 <sup>b</sup>	>10,000	16.0	2.79	1.87
30 <sup>b</sup>	>10,000	44.8	2.35	2.95
31 <sup>b</sup>	>10,000	41.9	2.38	3.08
32 <sup>a</sup>	510	21.5	1.38	2.00
33 <sup>b</sup>	>10,000	8.8	3.05	2.81
34 <sup>b</sup>	>10,000	8.0	3.10	2.66
35 <sup>b</sup>	>10,000	7.3	3.14	2.32
36 <sup>b</sup>	900	16.9	1.74	1.91
37 <sup>b</sup>	>10,000	56.6	2.27	2.18
38 <sup>b</sup>	3210	49.8	1.81	1.61
39 <sup>b</sup>	>10,000	4.4	3.35	2.50
40 <sup>b</sup>	1220	6.3	2.30	1.94
41 <sup>a</sup>	640	3.4	2.28	2.15
42 <sup>b</sup>	996	14.3	1.82	2.11
43 <sup>a</sup>	5.6	1.7	0.52	0.38
44 <sup>b</sup>	28	20.0	0.15	0.94
45 <sup>b</sup>	14	1.3	1.05	0.95
46 (L759656) <sup>a</sup>	4888	11.8	2.26	2.46
47 (L759633) <sup>a</sup>	1043	6.4	2.21	2.09
48 <sup>b</sup>	8.3	3.9	0.34	0.99
49 <sup>a</sup>	0.5	0.2	0.43	0.41
50 <sup>b</sup>	1.8	1.3	0.19	1.49
51 <sup>a</sup>	11.7	9.4	0.09	0.13
52 (O-1057) <sup>a</sup>	8.4	8.0	0.02	0.03
53 (AMG41) <sup>a</sup>	1.00	0.9	0.07	0.42
54 (JWH-133) <sup>a</sup>	677	3.4	2.30	2.19
55 (CP-55,490) <sup>a</sup>	0.6	0.6	0.00	0.07
56 (AM855) <sup>a</sup>	22.3	5.4	0.60	0.53
57 (BAY593074) <sup>a</sup>	48.3	45.5	0.03	-0.09
58 (WIN55212-2) <sup>b</sup>	13.3	1.3	1.01	1.88
59 (gp1a) <sup>a</sup>	363	0.04	3.95	4.20
60 <sup>b</sup>	1925	13.4	2.16	2.19
61 (SR144528) <sup>a</sup>	2890	5.4	2.74	2.83
62 (HU-308) <sup>a</sup>	10,000	22.7	2.64	2.85
63 (GW405833) <sup>a</sup>	1917	12.0	2.21	2.36
64 <sup>b</sup>	480	2.4	2.30	1.25

<sup>a</sup> Compound included in the training set.

<sup>b</sup> Compound included in the test set.

This visual representation of the contributions of **24** to the model highlights the great dominance of hydrophobic/non-polar cubes with respect to electron-withdrawing ones. In other words, selectivity appears to be strongly dependent on van der Waals

**Table 2**

3D-QSSR statistical parameters of the three phase-derived sets of models.

PLS	$r^{2a}$	SD <sup>b</sup>	F <sup>c</sup>	P <sup>d</sup>	RMSE <sup>e</sup>	Q <sup>2f</sup>	R-Pearson <sup>g</sup>
1	0.54	0.82	33.6	2.34e-06	0.61	0.56	0.75
2	0.89	0.39	118.5	1.60e-14	0.58	0.61	0.80
3	0.95	0.28	173.7	9.30e-18	0.57	0.63	0.81

<sup>a</sup>  $r^2$ : value of  $r^2$  for the regression.

<sup>b</sup> SD: standard deviation of the regression.

<sup>c</sup> F: variance ratio.

<sup>d</sup> P: significance level of variance ratio.

<sup>e</sup> RMSE: root-mean-square error.

<sup>f</sup> Q<sup>2</sup>: value of Q<sup>2</sup> for the predicted activities.

<sup>g</sup> R: r-Pearson, correlation between the predicted and observed selectivity index values for the test set.

interactions established by the adamantyl group on the amide moiety and by the C6 substituent (2-furyl group in compound **24**). In order for this ligand to keep these hydrophobic groups in the right orientation, the *trans*-conformation of the amide is required as well as the alignment of the amide carbonyl dipole with the ketone carbonyl dipole.

The 3D-QSSR model was then subjected to a prospective experimental validation. First of all, it was used to predict the selectivity of an external data set of 39 compounds reported in the literature [6,7c,10–12,19,25–27,43–50] (**E1–E39**, see Fig. 7 and Table S2 in the Supplementary material). The correlation coefficient ( $r^2 = 0.56$ ) of this unrelated set of derivatives was comparable to the value obtained for the test set; the linear plot of predicted versus actual selectivity index values (displayed in Fig. 2 and reported in the fifth and fourth columns of Table 3) and the differences between these values (within one order of magnitude for all the compounds with the exceptions of **E25** and **E29**); provided evidence that the correlation shown by the model was not a chance result.

Having gained such a confidence, as a second step, we tested the ability of our 3D-QSSR model to help the design of new CB2-selective ligands. Inspection of Fig. 3 clearly shows that the 8-position of

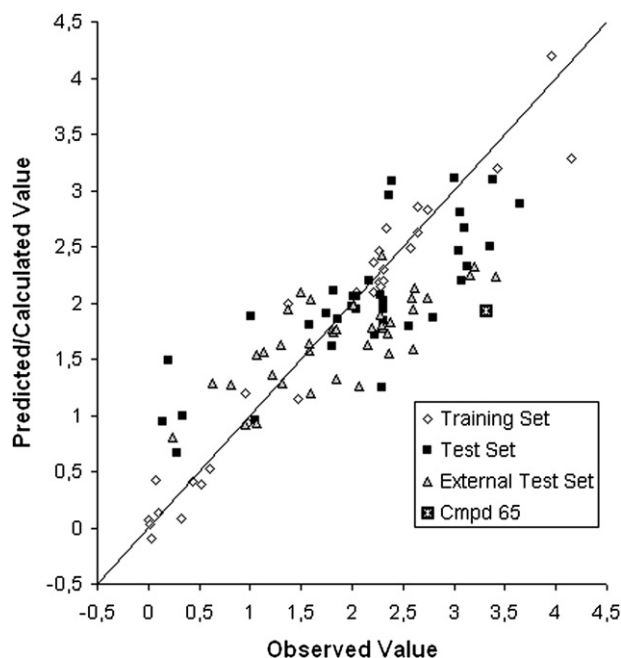


**Fig. 2.** Scatter plot for the predicted and observed selectivity index values [log(SI)] as calculated by the 3D-QSSR model applied to the training set, test set and external test set compounds.

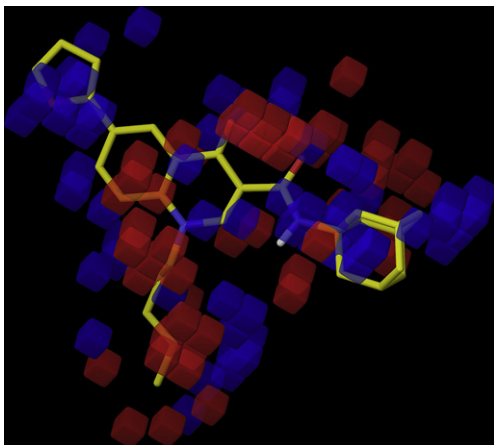


Fig. 3. Superposition of the 3D-QSSR model and the highly selective compound **24**.

the quinolone nucleus of compound **24** is surrounded by blue cubes, which suggests lipophilic substituents in this position might increase CB2 selectivity. Accordingly, based on our interest in studying the cannabinergic properties of quinolone derivatives, the *N*-(adamantan-1-yl)-4-oxo-8-methyl-1-pentyl-1,4-dihydroquinoline-3-carboxamide derivative (**65**) shown in Fig. 8 was considered as our synthetic test compound. The log(SI) value predicted by using our model (1.93, see Fig. 8) was indicative of high CB2 selectivity for such a compound, thus spurring us to synthesize it and to evaluate its CB1 and CB2 receptor affinity. The synthesis of **65** was carried out in 5 steps from *o*-toluidine according to a synthetic protocol previously utilized for the preparation of other quinolone derivatives [7c]. The synthesis of compound **65** is depicted in Scheme 1. The binding affinities of compounds **65** for human recombinant CB1 and CB2 receptors were evaluated in parallel with SR144528 [40] and rimonabant [51] as reference CB2 and CB1 ligands, respectively, as previously described [7c]. The new derivative was found to be an extremely selective CB2 ligand as it displayed high CB2 affinity ( $K_i = 4.9$  nM), while being devoid of CB1 affinity ( $K_i > 10,000$  nM), with a log(SI) value  $>3.3$ .

The comparison between the SI values of compounds **65** and **21** (8-unsubstituted analogue) demonstrates that the insertion of the small and lipophilic methyl group into the 8-position enhanced selectivity by approximately 200 fold, as a result of dramatic reduction in CB1 affinity.

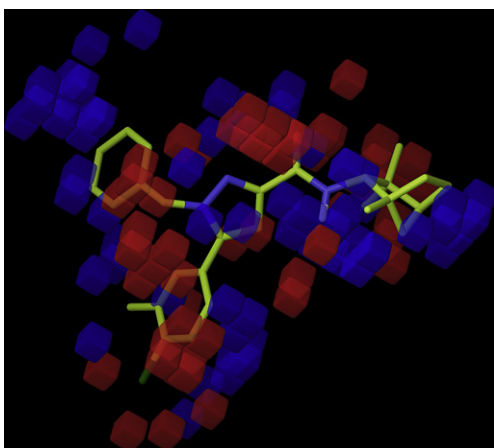


Fig. 4. Superposition of the 3D-QSSR model and the moderately selective compound **61** (SR144528).

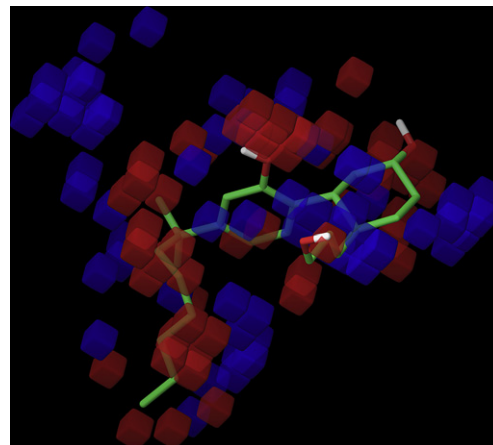


Fig. 5. Superposition of the 3D-QSSR model and the non selective compound **55** (CP-55,940).

### 3. Conclusion

The 3D computational model proposed in this study has been generated taking into account a number of structurally diverse compounds characterized by different selectivity index values and might be useful for the discovery of structurally novel selective CB2 ligands. Future studies should provide additional enhancements to the workflow here employed. Thus, exploiting the repeated appearance of new selective CB2 scaffolds in the literature, we are currently enlarging the ligands data set in an attempt to widen its inclusiveness.

In conclusion, the success of our computational strategy, which was prospectively tested by an unrelated test set of derivatives taken from the literature and led to the identification of one new selective CB2 receptor ligand, lends firm support for the practicality of quantitative ligand-based selectivity models for cannabinoid receptors. These drug discovery tools might represent a valuable complementary approach to docking studies performed on homology models of the receptors. Phase turned out to be an appropriate software package to achieve such a goal.

### 4. Methods

#### 4.1. Molecular modeling

Three-dimensional structure building, pharmacophore mapping and 3D-QSSR studies were carried out on an IBM workstation with Linux operating system running Maestro 8.0, MacroModel 9.5 and Phase 2.5 programs (Schrödinger, LLC, New York, NY). Phase, implemented in the Maestro modeling package, was used to generate pharmacophore and 3D-QSSR models for cannabinoid receptor CB2. The 3D structure of all the molecules used in Phase was built in Maestro. Conformers of each derivative were generated in MacroModel using the OPLS\_2005 force field, GB/SA water and no cutoff for nonbonded interactions. Molecular energy minimizations were performed using the PRGC method with 5000 maximum iterations and 0.001 gradient convergence threshold. The conformational searches were carried out by application of the MCMM torsional sampling method, performing automatic setup with 20 kJ/mol in the energy window for saving structure and a 0.5 Å cutoff distance for redundant conformers. Pharmacophore feature sites for the molecules were assigned using a set of features defined in Phase as hydrogen-bond acceptor (A), hydrogen-bond donor (D), hydrophobic group (H), negatively charged group (N),

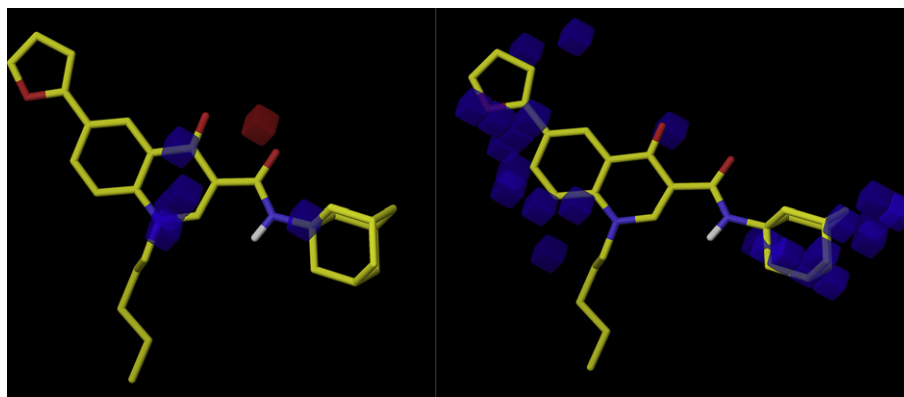


**Fig. 6.** Superpositions of the 3D-QSSR model and compound **24**. Only the cubes representing the model that are occupied by the compound are displayed (beyond the  $\pm 2.0 \times 10^{-2}$  threshold), decomposed into contributions by two different atom classes. Left: map corresponding to electron-withdrawing atoms (including hydrogen-bond acceptors). Right: map corresponding to hydrophobic/non-polar atoms. The blue and red cubes refer to regions in which CB2 selectivity is increased or decreased, respectively, by molecular occupancy. (For interpretation of the references to colour in this figure legend, the reader is referred to the web version of this article).

positively charged group (P), and aromatic ring (R). Four highly active compounds (**S1–S11–S26–S41**) were selected for generating the pharmacophore hypotheses for CB2 (Fig. S1 in the Supplementary material). Common pharmacophore hypotheses were identified using conformational analysis and a tree-based partitioning technique. The resulting pharmacophores were then

scored and ranked. The best-generated CB2 pharmacophore model (CB2PHAM) obtained by Phase consisted of five features: one hydrogen-bond acceptors (A; represent by red vectors), one aromatic groups (R; orange rings), three hydrophobic functions (H; green balls) (see Supplementary material for further details). This pharmacophore was chosen for further 3D-QSSR analysis. All the

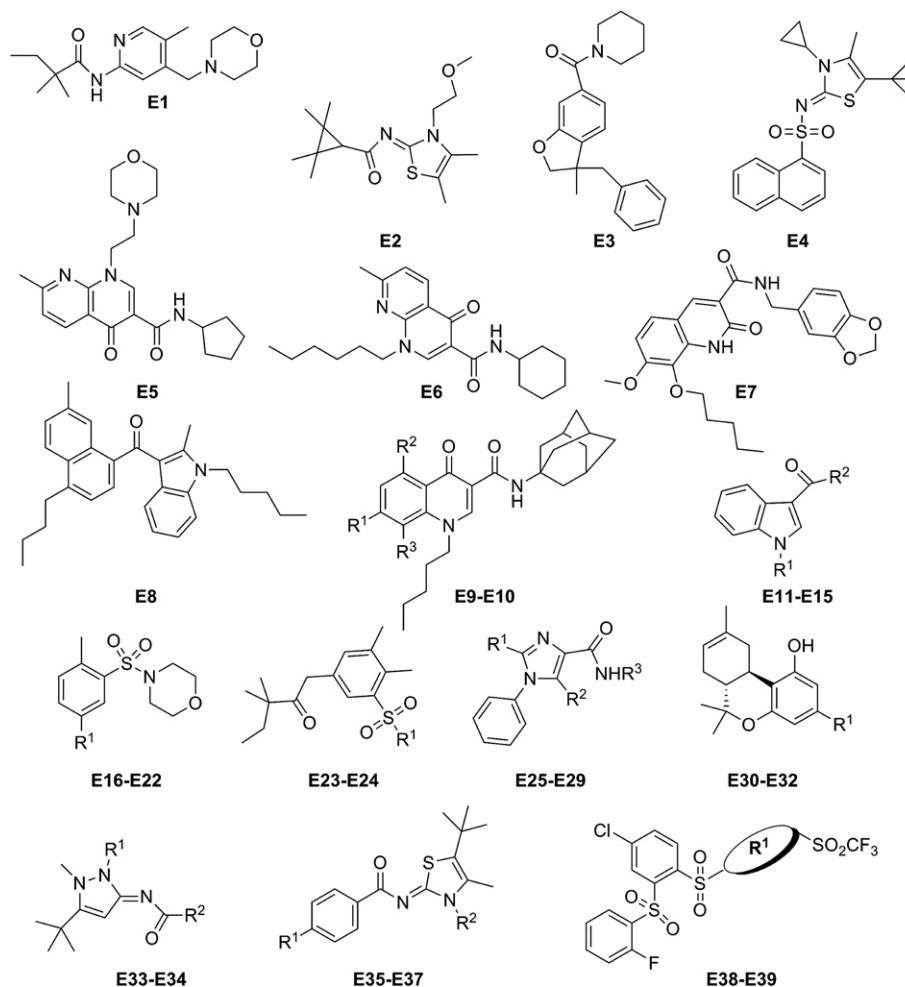


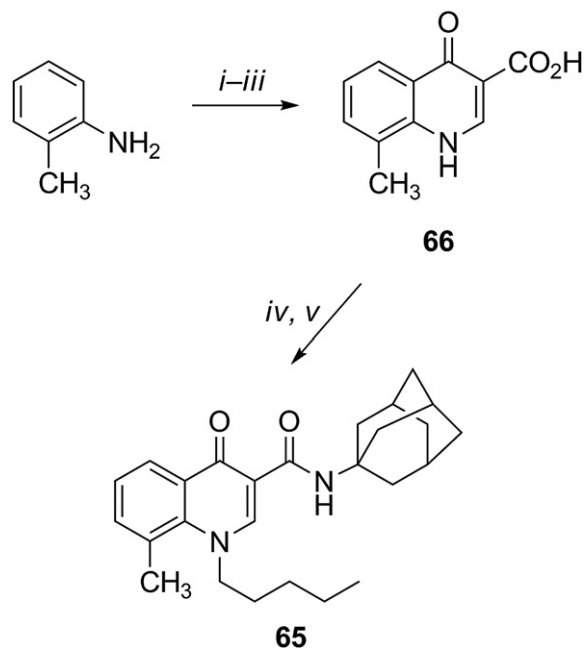
**Fig. 7.** Chemical scaffolds of the compounds included in the external test set (see Table S2 in the Supplementary material for further details).

**Table 3**

CB1 and CB2 receptor affinity values [ $K_i(\text{CB1})$  and  $K_i(\text{CB2})$  columns, nM], experimental (Exp column) and estimated (Calc column) selectivity index values [ $\log(\text{SI})$ ] for compounds of the external test set. Estimated  $\log(\text{SI})$  values were calculated by application of 3D-QSSR model (see text).

Cmpd	$K_i(\text{CB1})^a$	$K_i(\text{CB2})^a$	Exp $\log(\text{SI})$	Calc $\log(\text{SI})$
E1 [43]	3800	24	2.19	1.78
E2 [44]	270	0.64	2.62	2.13
E3 [45]	>10,000	422	1.37	1.94
E4 [46]	1700	16	2.02	1.98
E5 [25]	1000	50	1.30	1.63
E6 [25]	95	8	1.07	0.93
E7 [47]	2370	35.9	1.81	1.77
E8 [19]	42	6.5	0.81	1.27
E9 [7c]	2100	52.6	1.60	1.2
E10 [7c]	>10,000	25.5	2.59	2.04
E11 [11]	945	4.6	2.31	1.78
E12 [11]	616	16	1.58	1.64
E13 [11]	131	11	1.07	1.54
E14 [11]	220	3.3	1.82	1.74
E15 [11]	710	3.1	2.35	1.73
E16 [48]	130	3.9	1.5	2.09
E17 [48]	200	5.2	1.58	1.58
E18 [48]	390	23	1.22	1.36
E19 [48]	310	34	0.95	0.92
E20 [48]	790	11	1.85	1.32
E21 [48]	470	23	1.31	1.28
E22 [48]	3400	23	2.16	1.63
E23 [6]	1800	9	2.30	1.8
E24 [6]	650	2.7	2.38	1.93
E25 [10]	4152	1.6	3.41	2.23
E26 [10]	1995	9.8	2.3	2.43
E27 [10]	4887	2.7	3.2	2.32
E28 [10]	5444	9.7	2.74	2.05
E29 [10]	1422	3.5	2.6	1.59
E30 [26]	12.3	0.91	1.13	1.56
E31 [27]	1.86	1.05	0.24	0.8
E32 [27]	0.94	0.22	0.63	1.28
E33 [49]	1300	11	2.07	1.26
E34 [49]	870	3.7	2.37	1.55
E35 [50]	53	1.2	1.6	2.03
E36 [50]	1100	5.7	2.28	1.89
E37 [50]	4100	10	2.6	1.94
E38 [12]	2500	1.7	3.16	2.25
E39 [12]	560	8	1.84	1.76

<sup>a</sup> Binding affinities for human recombinant CB1 and CB2 receptors measured by displacement of radioligand [ $^3\text{H}$ ]-CP-55,940.



**Scheme 1.** Synthesis of compound 65. Reagents and conditions: i. EMME, 120 °C, 4 h; ii. diphenyl ether, reflux, 16 h; iii. 2.5 N NaOH, reflux, 4 h, then HCl; iv. 1-amino-adamantane, HOBT, HBTU, DIPEA, DMF, rt, 20 h; v. 1-iodopentane,  $\text{K}_2\text{CO}_3$ , DMF, 90 °C, 20 h.

molecules used for QSSR studies (Fig. 1) were aligned to the best pharmacophore hypothesis (CB2PHAM). Atom-based QSSR models were generated for CB2PHAM hypothesis using the 29-member training set and a grid spacing of 1.0 Å. QSSR models containing one to three PLS factors were generated.

#### 4.2. General chemistry

Reagents were obtained from commercial suppliers and used without further purifications. IR spectra were recorded on a Perkin–Elmer BX FT-IR system. TLC was carried out using Merck TLC plates Kieselgel 60 F254. Chromatographic purifications were performed on columns packed with Merck 60 silica gel, 23–400 mesh, for flash technique. Melting points were taken using a Gallenkamp

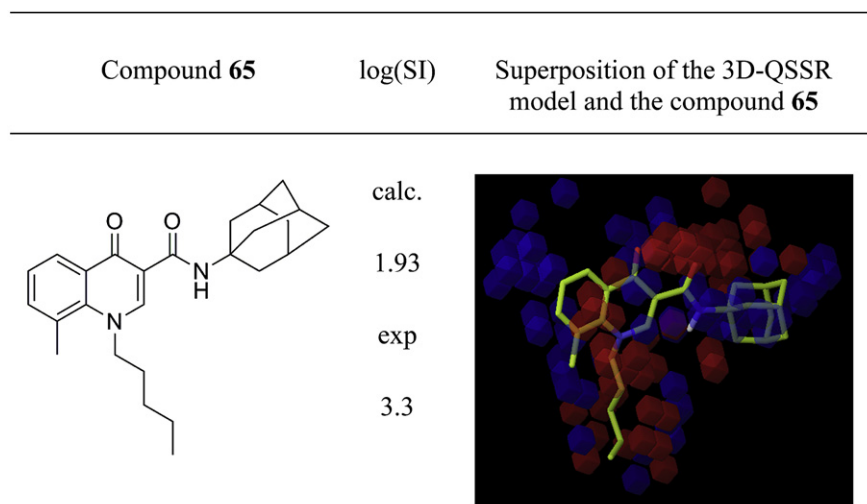


**Fig. 8.** Compound 65. Chemical structure, predicted selectivity index and superposition between the 3D-QSSR model and the putative bioactive conformation of this derivative.

melting point apparatus and are uncorrected.  $^1\text{H}$  NMR and  $^{13}\text{C}$  NMR spectra were recorded at 200 and 50 MHz, respectively, with a Bruker AC200F spectrometer, and chemical shifts are reported in  $\delta$  values, relative to TMS at  $\delta$  0.00 ppm. EI low-resolution MS spectra were recorded using an Agilent 1100 Series LC/MSD spectrometer with an electron beam of 70 eV. Elemental analyses (C, H, N) were performed in-house using a Perkin–Elmer Elemental Analyzer 240C.

#### 4.3. Synthesis of *N*-(adamantan-1-yl)-8-methyl-4-oxo-1-pentyl-1,4-dihydroquinoline-3-carboxamide (**65**)

A mixture of 2-methylaniline (1.07 g, 10 mmol) and diethyl ethoxymethylenemalonate (EMME) (2.16 g, 10 mmol) was heated at 120 °C for 4 h and cooled to room temperature. Diphenyl ether (15 mL) was added and the reaction mixture was heated at reflux temperature for 16 h. After cooling to room temperature, 2.5 N NaOH (20 mL, 50 mmol) was added and the reaction mixture was refluxed for 4 h. After cooling, 12 N HCl was added to the reaction mixture allowing the precipitation of the acid derivative, which was collected by filtration, washed with water, then petroleum ether, and recrystallized from ethanol to give 8-methyl-1,4-dihydroquinoline-4-one-3-carboxylic acid (**66**) as a beige solid (0.6 g, 30% overall yield):  $R_f = 0.45$  ( $\text{CH}_2\text{Cl}_2/\text{MeOH}$  95:5); mp: 254 °C;  $^1\text{H}$  NMR (200 MHz,  $\text{CDCl}_3$ ):  $\delta = 15.37$  (s, 1H), 8.61 (s, 1H), 8.12 (d,  $J = 8.0$  Hz, 1H), 7.70–7.65 (m, 1H), 7.46–7.40 (m, 2H), 2.50–2.45 ppm (m, 3H); IR ( $\text{CHCl}_3$ ):  $\nu = 1625, 1709\text{ cm}^{-1}$ ; MS (ESI, 70 eV)  $m/z$ : 204  $[\text{M} + \text{H}]^+$ ; Anal. calcd for  $\text{C}_{11}\text{H}_9\text{NO}_3$ : C 65.02, H 4.46, N 6.89, found: C 65.32, H 4.36, N 6.69.

The acid derivative **66** (408 mg, 2.0 mmol) was dissolved in dry DMF (10 mL) and HOBt (260 mg, 2.0 mmol), HBTU (1.52 g, 4.0 mmol), DIPEA (0.4 mL, 3.0 mmol) and 1-aminoadamantane (360 mg, 2.4 mmol) were added to the solution. After stirring at room temperature for 30 min, more DIPEA (0.4 mL, 3.0 mmol) was added and the reaction mixture was stirred at room temperature for 20 h.  $\text{K}_2\text{CO}_3$  (1.39 g, 10 mmol) and *n*-pentyl iodide (1.43 mL, 10 mmol) were added to the reaction mixture, which was heated at 90 °C for 20 h, then poured into ice and extracted with AcOEt. The organic layers were washed with brine, dried over anhydrous  $\text{Na}_2\text{SO}_4$  and evaporated to dryness. The crude residue was purified by flash column chromatography using  $\text{CH}_2\text{Cl}_2/\text{MeOH}$  97:3 as the eluent to afford the title compound **65** as a white solid (128 mg, 17% overall yield), which was recrystallized from ethanol:  $R_f = 0.78$  ( $\text{CH}_2\text{Cl}_2/\text{MeOH}$  97:3); mp: 140 °C;  $^1\text{H}$  NMR (200 MHz,  $\text{CDCl}_3$ ):  $\delta = 9.87$  (s, 1H), 8.66 (s, 1H), 8.49–8.40 (m, 1H), 7.45–7.40 (m, 1H), 7.34–7.30 (m, 1H), 4.36 (t,  $J = 7.7$  Hz, 2H), 2.73 (s, 3H), 2.12–2.07 (m, 9H), 1.71–1.65 (m, 8H), 1.24–1.20 (m, 4H), 0.83 ppm (t,  $J = 6.3$  Hz, 3H);  $^{13}\text{C}$  NMR (50 MHz,  $\text{CDCl}_3$ ):  $\delta = 13.8, 22.2, 23.8, 28.3, 29.6, 30.7, 36.6, 41.8, 51.6, 57.5, 112.7, 124.9, 126.0, 126.2, 129.9, 137.4, 139.5, 150.1, 163.6, 176.8$  ppm; IR ( $\text{CHCl}_3$ ):  $\nu = 1657\text{ cm}^{-1}$ ; MS (ESI, 70 eV)  $m/z$ : 407  $[\text{M} + \text{H}]^+$ ; Anal. calcd for  $\text{C}_{26}\text{H}_{34}\text{N}_2\text{O}_2$ : C 76.81, H 8.43, N 6.89, found: C 76.51, H 8.58, N 7.09.

#### 4.4. Biology

CB1 and CB2 binding assays: receptor binding assays were performed exactly as described previously [7c], using membranes of cells over-expressing the human recombinant CB1 or CB2 receptors.

#### Acknowledgements

Authors from the University of Siena gratefully acknowledge financial support from Siena Biotech S. p. A. Authors from CNR,

Pozzuoli, are very grateful to Mr. Marco Allarà for technical assistance.

#### Appendix. Supplementary data

Supplementary data associated with this article can be found, in the online version, at doi:10.1016/j.ejmech.2010.11.034.

#### References

- (a) L.A. Matsuda, S.J. Lolait, M.J. Brownstein, A.C. Young, T.I. Bonner, *Nature* 346 (1990) 561–564; (b) S. Munro, K.L. Thomas, M. Abu-Shaar, *Nature* 365 (1993) 61–65.
- V. Di Marzo, M. Bifulco, L. De Petrocellis, *Nat. Rev. Drug Discov.* 3 (2004) 771–784.
- (a) J. Fernández-Ruiz, J. Romero, G. Velasco, R.M. Tolón, J.A. Ramos, M. Guzmán, *Trends Pharmacol. Sci.* 28 (2007) 39–45; (b) G. Kunos, D. Osei-Hyiaman, S. Bátkai, K.A. Sharkey, A. Makriyannis, *Trends Pharmacol. Sci.* 30 (2009) 1–7.
- (a) V. Di Marzo, *Nat. Rev. Drug Discov.* 7 (2008) 438–455; (b) P. Pacher, S. Bátkai, G. Kunos, *Pharmacol. Rev.* 58 (2006) 389–462.
- R.G. Pertwee, A. Thomas, Therapeutic applications for agents that act at CB1 and CB2 receptors. in: P.H. Reggio (Ed.), *The Cannabinoid Receptors*. Humana Press, Totowa, 2009, pp. 361–392.
- I. Sellitto, B.L. Le Bourdonnec, K. Worm, A. Goodman, M.A. Savolainen, G.H. Chu, C.W. Ajello, C.T. Saeui, L.K. Leister, J.A. Casse, R.N. DeHaven, C.J. LaBuda, M. Koblish, P.J. Little, B.L. Brogdon, S.A. Smith, R.E. Dolle, *Bioorg. Med. Chem. Lett.* 20 (2010) 387–391.
- (a) R.J. Gleave, P.J. Beswick, A.J. Brown, G.M.P. Giblin, P. Goldsmith, C.P. Haslam, W.L. Mitchell, N.H. Nicholson, L.W. Page, S. Patel, S. Roomans, B.P. Slingsby, M.E. Swarbrick, *Bioorg. Med. Chem. Lett.* 20 (2010) 465–468; (b) M.G. Cascio, D. Bolognini, R.G. Pertwee, E. Palazzo, F. Corelli, S. Pasquini, V. Di Marzo, S. Maione, *Pharmacol. Res.* 61 (2010) 349–354; (c) S. Pasquini, L. Botta, T. Semeraro, C. Mugnaini, A. Ligresti, E. Palazzo, S. Maione, V. Di Marzo, F. Corelli, *J. Med. Chem.* 51 (2008) 5075–5084.
- G.M.P. Giblin, C.T. O'Shaughnessy, A. Naylor, W.L. Mitchell, A.J. Eatherton, B.P. Slingsby, D.A. Rawlings, P. Goldsmith, A.J. Brown, C.P. Haslam, N.M. Clayton, A.W. Wilson, I.P. Chessell, A.R. Wittington, R. Green, *J. Med. Chem.* 50 (2007) 2597–2600.
- R.G. Pertwee, *Br. J. Pharmacol.* 156 (2009) 397–411.
- J.H.M. Lange, M.A.W. van der Neut, H.C. Wals, G.D. Kuil, A.J.M. Borst, A. Mulder, A.P. den Hartog, H. Zilaout, W. Goutier, H.H. van Stuivenberg, B.J. van Vliet, *Bioorg. Med. Chem. Lett.* 20 (2010) 1084–1089.
- J.M. Frost, M.J. Dart, K.R. Tietje, T.R. Garrison, J.K. Grayson, A.V. Daza, O.F. El-Kouhen, B.B. Yao, G.C. Hsieh, M. Pai, C.Z. Zhu, P. Chandran, M.D. Meyers, *J. Med. Chem.* 53 (2010) 295–315.
- E.J. Gilbert, G. Zhou, M.K.C. Wong, L. Tong, B.B. Shankar, C. Huang, J. Kelly, B.J. Lavey, S.W. McCombie, L. Chen, R. Rizvi, Y. Dong, Y. Shu, J.A. Kozlowski, N.Y. Shih, W. Hipkin, W. Gonsiorek, A. Malikzay, C.A. Lunn, L. Favreau, D.J. Lundell, *Bioorg. Med. Chem. Lett.* 20 (2010) 608–611.
- (a) S. Durdagi, M.G. Papadopoulos, P.G. Zoumpoulakis, C. Koukoulitsa, T.A. Mavromoustakos, *Mol. Divers.* 14 (2010) 257–276; (b) E.K. Tiburu, S. Tyukhtenko, L. Deshmukh, O. Vinogradova, D.R. Janero, A. Makriyannis, *Biochem. Biophys. Res. Commun.* 384 (2009) 243–248; (c) E. Cichero, S. Cesarini, L. Mosti, P. Fossa, *J. Mol. Model.* 16 (2010) 677–691; (d) J.Z. Chen, X.W. Han, A. Makriyannis, J. Wang, X.Q. Xie, *J. Med. Chem.* 49 (2006) 625–636; (e) A.M. Ferreira, M. Krishnamurthy, B.M. Moore II, D. Finkelstein, D. Bashford, *Bioorg. Med. Chem.* 17 (2008) 2598–2606; (f) K. Worm, R.E. Dolle, *Curr. Pharm. Des.* 15 (2009) 3345–3366.
- P. Markt, C. Feldmann, J.M. Rollinger, S. Raduner, D. Schuster, J. Kirchmair, S. Distinto, G.M. Spitzer, G. Wolber, C. Laggner, K.H. Altmann, T. Langer, J. Gertsch, *J. Med. Chem.* 52 (2009) 369–378.
- G.B.L. De Freitas, L.L. da Silva, N.C. Romeiro, C.A.M. Fraga, *Eur. J. Med. Chem.* 44 (2009) 2482–2496.
- A. Weber, M. Böhm, C.T. Supuran, A. Scozzafava, C.A. Sottriffer, G. Klebe, *J. Chem. Inf. Model.* 46 (2006) 2737–2760.
- M. Fichera, G. Cruciani, A. Bianchi, G. Musumarra, *J. Med. Chem.* 43 (2000) 2300–2309.
- J.L. Wiley, I.D. Beletskaya, E.W. Ng, Z. Dai, P.J. Crocker, A. Mahadevan, R.K. Radzan, B.R. Martin, *J. Pharmacol. Exp. Ther.* 301 (2002) 679–689.
- J.W. Huffman, G. Zengin, M.J. Wu, G. Hynd, K. Bushell, A.L. Thompson, S. Bushell, C. Tartal, D.P. Hurst, P.H. Reggio, D.E. Shelley, M.P. Cassidy, J.L. Wiley, B.R. Martin, *Bioorg. Med. Chem.* 13 (2005) 89–112.
- R. Silvestri, M.G. Cascio, G. La Regina, F. Piscitelli, A. Lavecchia, A. Brizzi, S. Pasquini, M. Botta, E. Novellino, V. Di Marzo, F. Corelli, *J. Med. Chem.* 51 (2008) 1560–1576.
- S. Durdagi, A. Kapou, A. Kourouli, T. Andreou, S.P. Nikas, V.R. Nahmias, D.P. Papahatjis, M.G. Papadopoulos, T. Mavromoustakos, *J. Med. Chem.* 50 (2007) 2875–2885.
- D.P. Papahatjis, S.P. Nikas, T. Andreou, A. Makriyannis, *Bioorg. Med. Chem. Lett.* 12 (2002) 3583–3586.

- [23] J.W. Huffman, J. Liddle, S. Yu, M.M. Aung, M.E. Abood, J.L. Wiley, B.R. Martin, *Bioorg. Med. Chem.* 7 (1999) 2905–2914.
- [24] A.D. Khanolkar, D. Lu, P. Fan, X. Tian, A. Makriyannis, *Bioorg. Med. Chem. Lett.* 9 (1999) 2119–2124.
- [25] P.L. Ferrarini, V. Calderone, T. Cavallini, C. Manera, G. Saccomanni, L. Pani, S. Ruiu, G.L. Gessa, *Bioorg. Med. Chem.* 12 (2004) 1921–1933.
- [26] M. Krishnamurthy, S. Gurley, B.M. Moore II, *Bioorg. Med. Chem.* 16 (2008) 6489–6500.
- [27] A.K. Nadipuram, M. Krishnamurthy, A.M. Ferreira, W. Li, B.M. Moore II, *Bioorg. Med. Chem.* 11 (2003) 3121–3132.
- [28] J.M. Frost, M.J. Dart, K.R. Tietje, T.R. Garrison, G.K. Grayson, A.V. Daza, O.F. El-Kouhen, L.N. Miller, L. Li, B.B. Yao, G.C. Hsieh, M. Pai, C.Z. Zhu, P. Chandran, M.D. Meyer, *J. Med. Chem.* 51 (2008) 1904–1912.
- [29] S.L. Dixon, A.M. Smondyrev, E.H. Knoll, S.N. Rao, D.E. Shaw, R.A. Friesner, *J. Comput. Aided Mol. Des.* 20 (2006) 647–671.
- [30] Phase, Version 2.5, User Manual. Schrödinger Press, LLC, New York, 2005.
- [31] S. Pasquini, A. Ligresti, C. Mugnaini, T. Semeraro, L. Cicione, M. De Rosa, F. Guida, L. Luongo, M. De Chiaro, M.G. Cascio, D. Bolognini, P. Marini, R. Pertwee, S. Maione, V. Di Marzo, F. Corelli, *J. Med. Chem.* 53 (2010) 5915–5928.
- [32] R.G. Pertwee, *Curr. Med. Chem.* 6 (1999) 635–664.
- [33] M.M. Ibrahim, H. Deng, A. Zvonok, D.A. Cockayne, J. Kwan, H.P. Mata, T.W. Vanderah, J. Lai, F. Porreca, A. Makriyannis, T.P. Malan Jr., *Proc. Natl. Acad. Sci. U.S.A.* 100 (2003) 10529–10533.
- [34] R.A. Ross, H.C. Brockie, L.A. Stevenson, V.L. Murphy, F. Templeton, A. Makriyannis, R.G. Pertwee, *Br. J. Pharmacol.* 126 (1999) 665–672.
- [35] K. Worm, D.G. Weaver, R.C. Green, C.T. Saeui, D.M.S. Dulay, W.M. Barker, J.A. Cassel, G.J. Stabley, R.N. DeHaven, C.J. LaBuda, M. Koblish, B.L. Brogdon, S.A. Smith, R.E. Dolle, *Bioorg. Med. Chem. Lett.* 19 (2009) 5004–5008.
- [36] R.G. Pertwee, T.M. Gibson, L.A. Stevenson, R.A. Ross, W.K. Banner, B. Saha, R.K. Razdan, B.R. Martin, *Br. J. Pharmacol.* 129 (2000) 1577–1584.
- [37] J. De Vry, D. Denzer, E. Reissmueller, M. Eijckenboom, M. Heil, H. Meier, F. Mauler, *J. Pharmacol. Exp. Ther.* 310 (2004) 620–632.
- [38] G. Murineddu, P. Lazzari, S. Ruiu, A. Sanna, G. Loriga, I. Manca, M. Falzoi, C. Dessì, M.M. Curzu, G. Chelucci, L. Pani, G.A. Pinna, *J. Med. Chem.* 49 (2006) 7502–7512.
- [39] E. Stern, G.G. Muccioli, R. Millet, J.F. Goossens, A. Farce, P. Chavatte, J.H. Poupaert, D.M. Lambert, P. Depreux, J.P. Hénichart, *J. Med. Chem.* 49 (2006) 70–79.
- [40] M. Rinaldi-Carmona, F. Barth, J. Millan, J.M. Derocq, P. Casellas, C. Congy, D. Oustric, M. Sarran, M. Bouaboula, B. Calandra, M. Portier, D. Shire, J.C. Breliere, G.L. Le Fur, *J. Pharmacol. Exp. Ther.* 284 (1998) 644–650.
- [41] L. Hanus, A. Breuer, S. Tchilibon, S. Shiloah, D. Goldenberg, M. Horowitz, R.G. Pertwee, R.A. Ross, R. Mechoulam, E. Frider, *Proc. Natl. Acad. Sci. U.S.A.* 96 (1999) 14228–14233.
- [42] K.J. Valenzano, L. Tafesse, G. Lee, J.E. Harrison, J.M. Boulet, S.L. Gottshall, L. Mark, M.S. Pearson, W. Miller, S. Shan, L. Rabadi, Y. Rotshteyn, S.M. Chaffer, P.I. Turchin, Y. Elsemore, M. Toth, L. Koetzner, G.T. Whiteside, *Neuropharmacology* 48 (2005) 658–672.
- [43] G.H. Chu, C.T. Saeui, K. Worm, D.G. Weaver, A.J. Goodman, R.L. Broadrup, J.A. Cassel, R.N. DeHaven, C.J. LaBuda, M. Koblish, B. Brogdon, S. Smith, B. Le Bourdonnec, R.E. Dolle, *Bioorg. Med. Chem. Lett.* 20 (2009) 5931–5935.
- [44] B.B. Yao, G. Hsieh, A.V. Daza, Y. Fan, G.K. Grayson, T.R. Garrison, O. El Kouhen, B.A. Hooker, M. Pai, E.J. Wensink, A.K. Salyers, P. Chandran, C.Z. Zhu, C. Zhong, K. Ryther, M.E. Gallagher, C.L. Chin, A.E. Tovcimak, V.P. Hradil, G.B. Fox, M.J. Dart, P. Honore, M.D. Meyer, *J. Pharmacol. Exp. Ther.* 1 (2009) 141–151.
- [45] M. Naguib, P. Diaz, J.J. Xu, F. Astruc-Diaz, S. Craig, P. Vivas-Mejia, D.L. Brown, *Br. J. Pharmacol.* 7 (2008) 1104–1116.
- [46] H. Ohta, T. Ishizaka, M. Yoshinaga, A. Morita, Y. Tomishima, Y. Toda, S. Saito, *Bioorg. Med. Chem. Lett.* 17 (2007) 5133–5135.
- [47] H. Iwamura, H. Suzuki, Y. Ueda, T. Kaya, T. Inaba, *J. Pharmacol. Exp. Ther.* 296 (2001) 420–425.
- [48] A.J. Goodman, C.V. Ajello, K. Worm, B. Le Bourdonnec, M.A. Savolainen, H. O'Hare, J.A. Cassel, G.J. Stabley, R.N. DeHaven, C.J. LaBuda, M. Koblish, P.J. Little, B.L. Brogdon, S.A. Smith, R.E. Dolle, *Bioorg. Med. Chem. Lett.* 19 (2009) 309–313.
- [49] H. Ohta, T. Ishizaka, M. Tatsuzuki, M. Yoshinaga, I. Iida, T. Yamaguchi, Y. Tomishima, N. Futaki, Y. Toda, S. Saito, *Bioorg. Med. Chem.* 16 (2008) 1111–1124.
- [50] H. Ohta, T. Ishizaka, M. Tatsuzuki, M. Yoshinaga, I. Iida, Y. Tomishima, Y. Toda, S. Saito, *Bioorg. Med. Chem. Lett.* 17 (2007) 6299–6304.
- [51] (a) M. Rinaldi-Carmona, F. Barth, M. Héaulme, D. Shire, B. Calandra, C. Congy, S. Martinez, J. Maruani, G. Néliat, D. Caput, P. Ferrara, P. Soubrié, J.C. Brelière, G. Le Fur, *FEBS Lett.* 350 (1994) 240–244;  
(b) L.A. Sorbera, J. Castaner, J.S. Silvestre, *Drugs Future* 30 (2005) 128–137.